

E1-2009-188

S. Vokál<sup>1,\*</sup>, J. Vrláková<sup>1</sup>

RELATIVISTIC PARTICLES PRODUCED IN  $^{208}\text{Pb}$   
INDUCED NUCLEAR COLLISIONS AT 158 A GeV/c

Submitted to «Ядерная физика»

---

<sup>1</sup>P. J. Šafárik University, Košice, Slovakia

\*E-mail: stanislav.vokal@upjs.sk

Вокал С., Врлакова Я.

E1-2009-188

Релятивистские частицы, рожденные в ядерных соударениях ядер  $^{208}\text{Pb}$  с импульсом 158 АГэВ/с

Представлены результаты исследования угловой структуры частиц, рожденных во взаимодействиях ядер  $^{208}\text{Pb}$  с импульсом 158 АГэВ/с с ядрами Ag(Br) в фотоэмульсии. Используются три разных метода анализа (факториальные моменты, вейвлет-анализ и параметр  $S_2$ ). Обнаружены нестатистические флуктуации при использовании метода факториальных моментов в пространстве псевдобыстрот. Проведен сравнительный анализ с данными, полученными в рамках единого подхода при других энергиях и массах ядер пучка и при разной степени центральности Pb-событий. Не найден минимум в зависимости параметра  $\lambda_q$  от  $q$ . Приведены некоторые результаты исследования распределений по псевдобыстроте рожденных частиц методом непрерывного вейвлет-анализа. Найден нерегулярности в вейвлетных спектрах при шкалах  $a \leq 0,5$ , которые можно интерпретировать как псевдобыстроты приоритетного испускания групп частиц. Зарегистрированы нестатистические кольцевые структуры рожденных частиц в азимутальной плоскости взаимодействия, и определены их параметры с использованием  $S_2$ -метода.

Работа выполнена в Лаборатории физики высоких энергий им. В. И. Векслера и А. М. Балдина ОИЯИ.

Препринт Объединенного института ядерных исследований. Дубна, 2009

Vokál S., Vrláková J.

E1-2009-188

Relativistic Particles Produced in  $^{208}\text{Pb}$  Induced Nuclear Collisions at 158 A GeV/c

The angular structures of relativistic particles produced in  $^{208}\text{Pb} + \text{Ag}(\text{Br})$  collisions in emulsion detector at 158 A GeV/c have been studied. Three different methods of analysis have been used — scaled factorial moments, wavelets and parameter  $S_2$ . An evidence for nonstatistical fluctuations has been shown using the method of scaled factorial moments in pseudorapidity phase space. The comparative study has been done for different beam energies and masses and Pb + Em events with different degree of centrality. No clear minimum has been found in the dependences of intermittency parameter  $\lambda_q$  on  $q$ . The continuous wavelet transform has been applied to the pseudorapidity spectra of produced particles. Some irregularities have been revealed mainly in the scale range  $a \leq 0.5$  which can be interpreted as the preferred pseudorapidities of groups of emitted particles. The nonstatistical ring-like structures of produced particles in azimuthal plane of a collision have been found and their parameters have been determined when the azimuthal structures of produced particles have been investigated using the  $S_2$  method.

The investigation has been performed at the Veksler and Baldin Laboratory of High Energy Physics, JINR.

Preprint of the Joint Institute for Nuclear Research. Dubna, 2009

## 1. INTRODUCTION

One of the topics intensively investigated in nuclear collisions at high energies is to search for phenomena connected with large densities obtained in such interactions. The existence of quark–gluon plasma (QGP) have been predicted in the framework of the quantum chromodynamics. As an example, the transition from the QGP back to the normal hadronic phase was predicted to give large fluctuations in the number of produced particles in local regions of phase space [1, 2].

The goal of our work was to present our last results obtained when some peculiarities in the emission of relativistic particles produced in  $^{208}\text{Pb} + \text{Ag}(\text{Br})$  interactions at  $158 \text{ A GeV}/c$  have been studied. There are many methods proposed to analyze such effects in relativistic interactions of two nuclei. Three methods have been used in our analysis:

- method of  $S_2$  parameter [3],
- wavelet method [4],
- scaled factorial moment method [5].

The  $S_2$ -parameter and wavelet methods are described and some selected results are discussed. The main aim of this paper is to present some new results of the search for fluctuations of relativistic particles produced in  $^{208}\text{Pb}$  induced interactions with  $\text{Ag}(\text{Br})$  targets at the CERN SPS energy using the method of scaled factorial moments.

Experimental sample was collected in the EMU12 experiment organized by the EMU01 Collaboration [6, 7]. Comparison of experimental data with model calculations for events with different degree of centrality and for different beam nuclei have been done using the modified FRITIOF [8, 9] and cascade models [10].

## 2. EXPERIMENT

Nuclear emulsions were irradiated horizontally by  $158 \text{ A GeV}/c$   $^{208}\text{Pb}$  beam at the CERN SPS — experiment EMU12. Experimental details can be found in [6, 7]. In the measured interactions all charged secondary particles were classified according to the commonly accepted emulsion experiment terminology into the following groups:

- $b$  particles (black) — singly and multi-charged fragments evaporated from the target;
- $g$  particles (grey) — charged particles with a range  $\geq 3$  mm,  $b$  and  $g$  particles are target fragments with  $\beta < 0.7$ ;
- $s$  particles — the relativistic particles with  $\beta \geq 0.7$  emitted outside the fragmentation cone, this group includes particles produced in the interactions as well as those knocked out from the target nucleus;
- $f$  particles — the projectile fragments with  $\beta \sim 0.99$ .

The schematic view of our experimental setup is shown in Fig. 1.

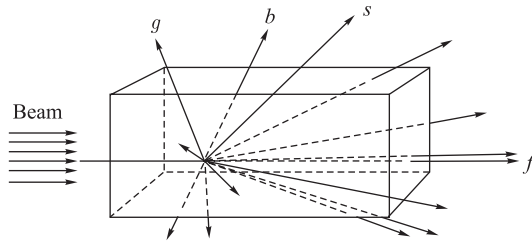


Fig. 1. Our experimental setup

The polar ( $\theta$ ) and azimuthal ( $\Psi$ ) emission angles of all tracks were measured. The pseudorapidity ( $\eta = -\ln \left[ \tan \frac{\theta}{2} \right]$ ) was calculated for each relativistic particle.

The event of  $^{208}\text{Pb}$  nuclear interaction in emulsion detector is presented in Fig. 2.

One can see the primary track of Pb nuclei on the left side and the tracks of produced particles, mainly fragments, on the right side.

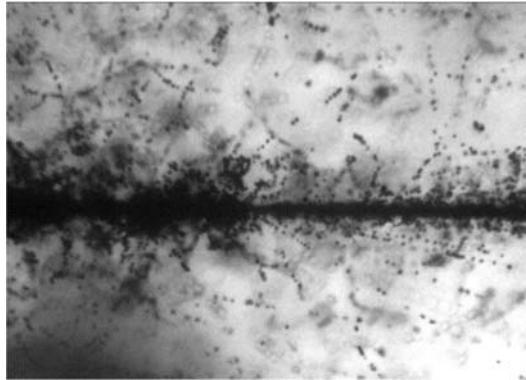


Fig. 2. The  $^{208}\text{Pb}$  interaction in emulsion detector at 158 A GeV/c

The dependence of the number of produced relativistic particles ( $N_s$ ) on the impact parameter  $b_{\text{imp}}$  calculated by the FRITIOF model for  $^{208}\text{Pb} + \text{Em}$  collisions at 158 A GeV/c is shown in Fig. 3 for different emulsion targets [11]. One can see that interactions with  $N_s > 350$  are those of lead nuclei with the heavy emulsion

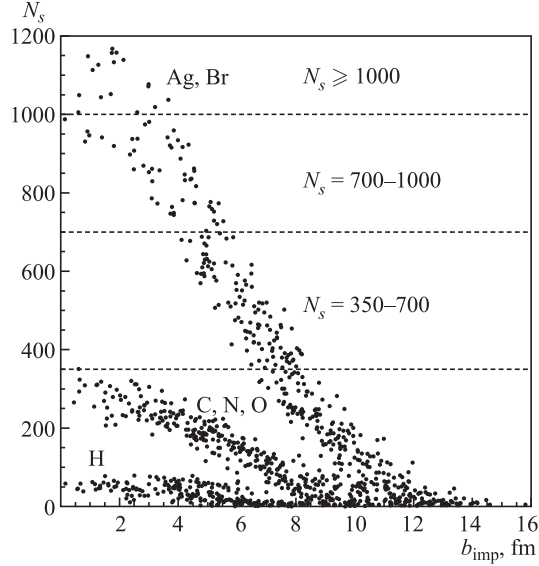


Fig. 3. The dependence of multiplicity of produced relativistic particles  $N_s$  on the impact parameter  $b_{\text{imp}}$  for  $^{208}\text{Pb} + \text{Em}$  collisions at  $158 \text{ A GeV}/c$  for different emulsion targets calculated by the FRITIOF model

targets Ag and Br. The group with  $N_s \geq 1000$  comprises the central Pb + Ag(Br) interactions with impact parameter  $b_{\text{imp}} \approx (0 - 2) \text{ fm}$ .

For the analysis 64 events with the number of relativistic particles  $N_s > 350$  have been selected from the total number of 628 minimum bias events of  $^{208}\text{Pb} + \text{Em}$  interactions at  $158 \text{ A GeV}/c$ .

### 3. METHODS OF ANALYSIS

In our previous investigations three different methods of analysis (the method of  $S_2$  parameter, wavelet analysis and the method of scaled factorial moments [3–5]) have been used. Two methods (wavelet and  $S_2$ -parameter) are described and some selected results are presented here. As was mentioned in the introduction, the main aim of this paper is to present some new results of the search for fluctuations of relativistic particles produced in  $^{208}\text{Pb}$  induced interactions with Ag(Br) targets at the CERN SPS energy made by the method of scaled factorial moments.

**3.1. Method of the  $S_2$  Parameter.** The method of  $S_2$  parameter was proposed by E. Stenlund (EMU01 Collaboration), and detailed study of the average values of the parameter  $S_2$  was done in [3].

The azimuthal substructure of particles produced in ultra-relativistic heavy-ion collisions was investigated. It was found out that the observed substructure seems to be of stochastic nature and the features of the experimental data can be understood when effects like gamma-conversion and particle interference (HBT) are taken into account.

How was it found out in [3]? When azimuthal distributions of particles from relativistic heavy-ion collisions, produced within a narrow region of pseudorapidity, are studied, two classes of spectra are seen (Fig. 4). The jet class consists of cases where several particles seem to form clusters in the azimuthal plane, clusters which are separated with rather large void regions, as sketched in Fig. 4, *a*. The ring class consists of cases where the particles are distributed almost regularly as the spokes in a wheel (Fig. 4, *b*).

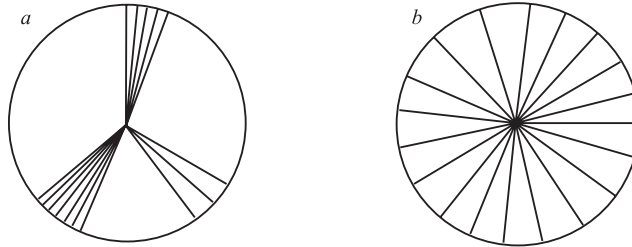


Fig. 4. Examples of two extreme azimuthal structures: (a) jet-like, (b) ring-like

In the  $S_2$  method [3] the multiplicity  $N_d$  of the analyzed subgroup from an individual event is kept fixed. Each  $N_d$  tuple of consecutive particles along the  $\eta$  axis of individual event can then be considered as a subgroup characterized by:

- a size  $\Delta\eta_d = \eta_{\max} - \eta_{\min}$ , where  $\eta_{\min}$  and  $\eta_{\max}$  are the pseudorapidity values of the first and last particles in the subgroup;
- density  $\rho_d = N_d/\Delta\eta_d$ ;
- average pseudorapidity (or subgroup position)  $\eta_m = \sum \eta_i/N_d$ .

To parametrize the azimuthal structure of the subgroup in a suitable way, a parameter  $S_2$  of the azimuthal structure has been suggested, where  $\Delta\phi$  is the difference between azimuthal angles of two neighboring particles in the investigated group (starting from the first and second and ending with the last and first):

$$S_2 = \sum (\Delta\phi_i)^2. \quad (1)$$

For the sake of simplicity,  $\Delta\phi$  was counted in units of full revolutions  $\Delta\phi_i = 1$ . The parameter  $S_2$  is small ( $S_2 \rightarrow 1/N_d$ ) for the particle groups with the ring-like structure and is large ( $S_2 \rightarrow 1$ ) for the particle groups with the jet-like structure.

The expectation value for the parameter  $S_2$ , in the case of a stochastic scenario with independent particles in the investigated group, can be analytically

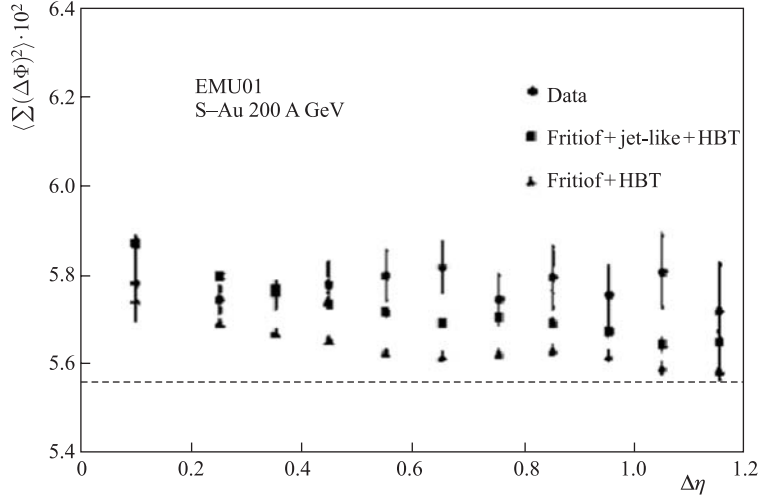


Fig. 5. The dependence of the parameter  $S_2$  on group size for central 200 A GeV S + Au interactions,  $N_s \geq 300$ ,  $N_d = 35$ . The dashed line indicates the expectation values for purely stochastic emission

expressed [3] as

$$\langle S_2 \rangle = \frac{2}{(N_d + 1)}. \quad (2)$$

This expectation value can be derived from the distribution of gaps between neighbors.

Figure 5 shows the results of the analysis of the generated FRITIOF+HBT sample, with and without  $\gamma$  conversion, compared with the results obtained from the data [3].

One can see that except for some additional jet structure seen by the  $S_2$  parameter for the dilute groups, the features of the data can be understood as a superposition of stochastic fluctuations,  $\gamma$  conversion and particle interference. Finally it was concluded in [3] that jet-like and ring-like events do not exhibit significant deviations from what can be expected from stochastic emission. But average value studies do not give a full information about an effect. Next step was performed in 2002 [12] where the systematic study of the  $S_2$  spectra for subgroups of the particles produced in  $^{197}\text{Au}$  induced collisions with heavy targets (Ag, Br) in emulsion detector has started. Nonstatistical ring-like substructures have been found and cone emission angles as well as other parameters have been determined.

What we can expect to see in the experimental  $S_2/\langle S_2 \rangle$  distributions in different scenarios was shown in 2004 [13]. It is illustrated schematically in Fig. 6 using, for example, Gauss distributions. In case of a pure stochastic scenario

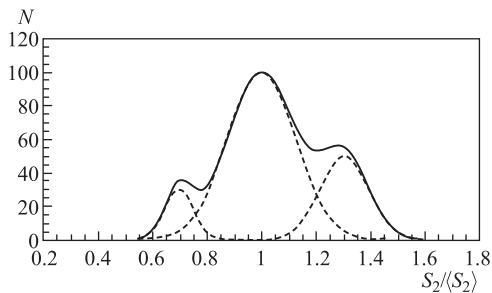


Fig. 6. The example of possible summary  $S_2/\langle S_2 \rangle$  distribution from three effects: stochastic + ring-like + jet-like effect distribution

the distribution would have a peak position at 1. The existence of the jet-like structures in collisions results in appearance of additional  $S_2$  distribution from this effect, but shifted to the right side in comparison with stochastic distribution. Analogously, the existence of the ring-like structures results in appearance of additions to  $S_2$  distribution from this effect, but shifted to the left side. As a result, the summary  $S_2$  distribution from these three effects may have

different form and depends on mutual order and sizes.

The experimental normalized  $S_2/\langle S_2 \rangle$  distributions have been compared with the distributions calculated by the FRITIOF model [14]. One of the results is shown in Fig. 7, *a, b*.

The model spectra were aligned according to the position of the peak with the experimental one. The FRITIOF includes neither the ring-like nor the jet-like effects, so the model spectra are used like the statistical background. Except this, in [3], it was shown that the  $S_2$  distribution for the FRITIOF model coincides with the calculated distribution in the case of the stochastic scenario with independent particles in the investigated group.

One can see that the experimental distributions are broader than the spectra calculated by the FRITIOF model. The experimental distributions have a surplus of events on both sides of the center. Such a situation takes place for all  $N_s$  and any  $N_d$  groups which were examined.

The results obtained from the experimental data after the subtraction of the statistical background are shown in Fig. 7, *c, d*. The obtained distributions have two very good distinguishable hills, the first in the region  $S_2/\langle S_2 \rangle < 1$ , where the ring-like effects are expected, and the second in the jet-like region ( $S_2/\langle S_2 \rangle > 1$ ).

The preliminary result is that the azimuthal structures of produced particles from collisions induced by the 158 A GeV/c  $^{208}\text{Pb}$  beams with Ag(Br) targets in the emulsion detector have been investigated and the additional groups of produced particles in the region of the ring-like structures ( $S_2/\langle S_2 \rangle < 1$ ) and the jet-like structures ( $S_2/\langle S_2 \rangle > 1$ ) in comparison to the FRITIOF model calculations have been observed [11, 14]. A similar situation has been observed in the interactions of 11 A GeV/c  $^{197}\text{Au}$  beams with heavy targets in the emulsion detector [13].

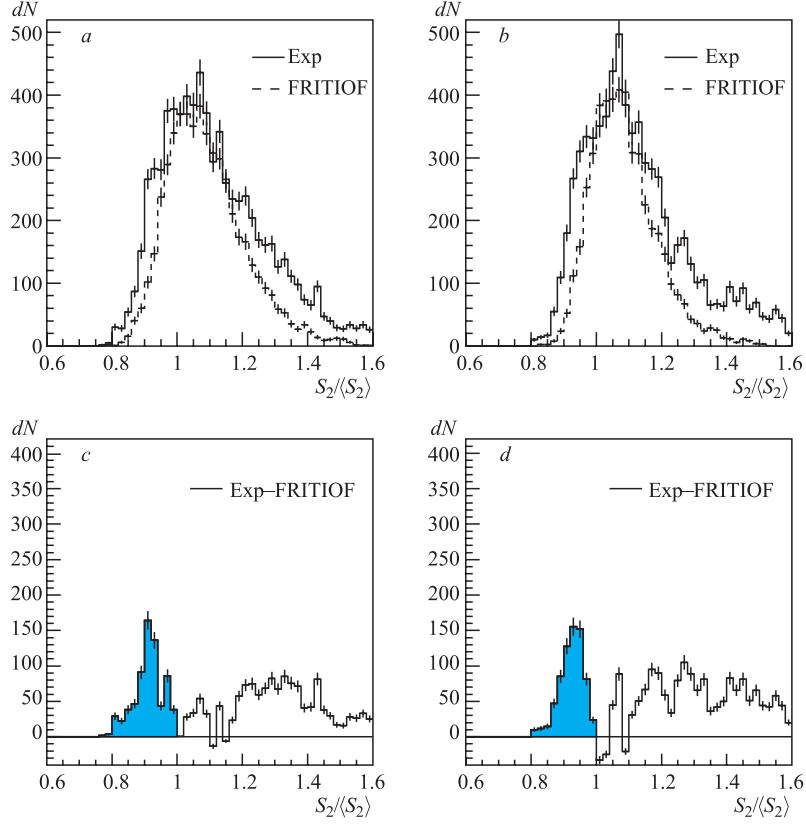


Fig. 7. The  $S_2/\langle S_2 \rangle$  distributions for  $^{208}\text{Pb} + \text{Ag}(\text{Br})$  collisions at 158 A GeV/c with  $N_s \geq 1000$ : the experimental one compared with FRITIOF model calculations for subgroup with (a)  $N_d = 60$  and (b)  $N_d = 90$ . The experimental  $S_2/\langle S_2 \rangle$  distributions after the subtraction of the FRITIOF ones for (c)  $N_d = 60$  and (d)  $N_d = 90$

**3.2. Wavelet Method.** The distributions of both the azimuthal and polar angles of produced particles have been investigated simultaneously to observe irregularities in particle emission. The continuous wavelet approach was applied to the angular spectra of the relativistic particles created in Au and Pb induced nuclear collisions at AGS and SPS energies [15, 16]. The wavelet pseudorapidity spectra have been subsequently surveyed at different scales to look for signs of ring-like structures. The particles contributing to the ring-like structures are expected to give peaks or bumps at certain typical pseudorapidities and to have approximately uniform azimuthal distributions (at certain scales).

Wavelet pseudorapidity spectrum of event is the sum of wavelets representing the individual particles. Wavelet coefficients  $W_\psi(a, b)$  reflect the probability to observe particle at some pseudorapidity  $b$  and scale  $a$ :

$$W_\psi(a, b) = \frac{1}{N} \sum_{i=1}^N a^{-1/2} \psi \left( \frac{\eta_i - b}{a} \right). \quad (3)$$

The second derivative  $g_2$  of Gaussian function (also known as Mexican hat) was chosen as a mother wavelet.

Wavelet  $g_2$  pseudorapidity spectra for all  $s$  particles at the three different scales  $a$  are presented in Fig. 8 [16].

The  $b_{\max}$  spectra plotted for the four different scale intervals are presented in Fig. 9 [16]. The scale intervals were introduced to investigate how an occurrence of maxima  $W_\psi(a_{\max}, b_{\max})$  depends on scale.

One can see that the local maximum referred to as irregularities were uncovered in the wavelet pseudorapidity distributions mainly in the scale range  $a \leq 0.5$ . These irregularities indicate the preferred pseudorapidities of groups of emitted particles.

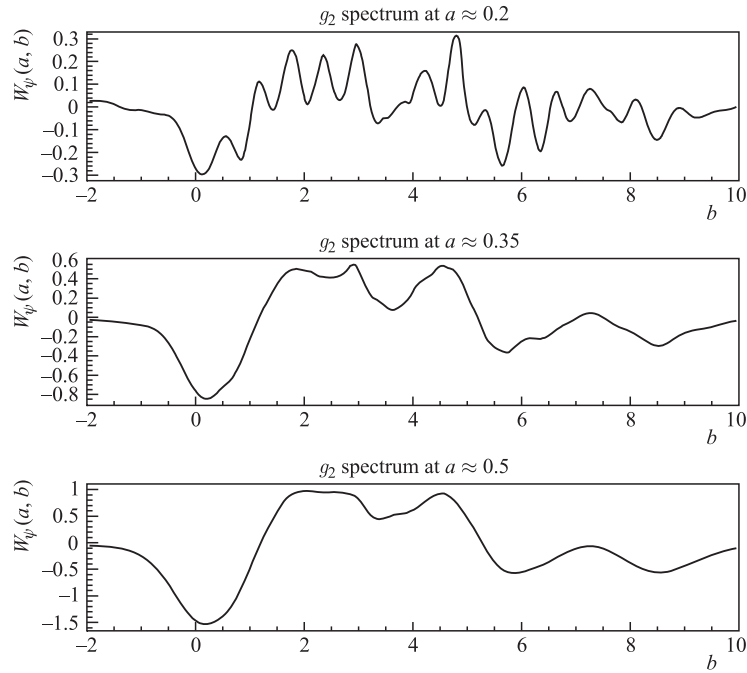


Fig. 8. Wavelet  $g_2$  pseudorapidity spectra of all the studied Pb events seen at the three different scales  $a$

### 3.3. Scaled Factorial Moments Method Analysis.

Experimental data on particle fluctuations in small space domains have been presented for various high-energy multiparticle collisions. Bialas and Peschanski [17, 18] suggested to study the dependence of factorial moments  $F_q$ , where  $q$  is the order of the moment, as a function of the bin width  $\delta\eta$ . The intermittent behaviour should lead to a power law dependence of the factorial moments on the bin size  $F_q \propto (\Delta\eta/\delta\eta)^{\varphi_q}$ ,  $\varphi_q > 0$ , where  $\Delta\eta$  is the pseudorapidity interval of produced relativistic particles.

Three methods: method of horizontal factorial moments (HFM), vertical factorial moments (VFM) and mixed factorial moments (MFM) have been proposed in [5]. The standard horizontal factorial moments  $F_e^{(H)}$  characterizing the  $e$ th event are defined by the following formula:

$$F_e^{(H)}(q) = M^{q-1} \sum_{m=1}^M \frac{F(n_{me}; q)}{[N_e^{(H)}]^q}, \quad (4)$$

where  $M$  is the number of equal bins of size  $\delta\eta$  into which the pseudorapidity interval  $\Delta\eta$  has been divided,  $n_{me}$  is the number of shower particles in the  $m$ th bin. Nonaveraging and nonnormalized factorial moments are given by  $F(n; q) = n(n-1)\dots(n-q+1)$ . Vertical averaging of  $F_e^{(H)}$  gives the full form

$$F^{(H)}(q) = \frac{1}{E} \sum_{e=1}^E F_e^{(H)}(q). \quad (5)$$

Denominator of the horizontal moment (4) is  $N_e^{(H)} = \sum_{m=1}^M n_{me}$ .

Vertical analysis is suggested in case of rare events with sharp peaks. In this case the normalized standard vertical moments characterizing the  $m$ th bin are

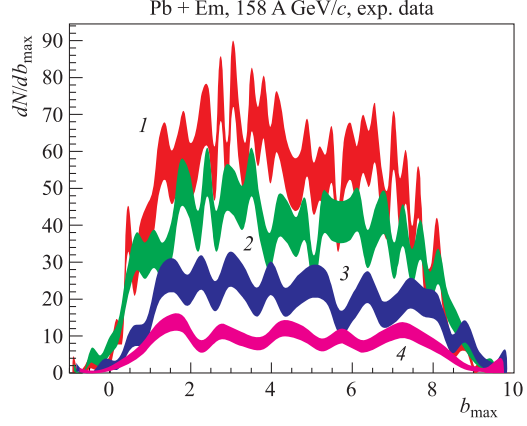


Fig. 9. The  $b_{\max}$  spectra of the experimental Pb+Em events seen in the four scale bands: 1)  $0.05 < a_{\max} \leq 0.1$ ; 2)  $0.1 < a_{\max} \leq 0.2$ ; 3)  $0.2 < a_{\max} \leq 0.3$ ; 4)  $0.3 < a_{\max} \leq 0.45$

given by

$$F_m^{(V)}(q) = E^{q-1} \sum_{e=1}^E \frac{F(n_{me}; q)}{[N_m^{(V)}]^q} \quad (6)$$

and the horizontal averaging gives the full form

$$F^{(V)}(q) = \frac{1}{M} \sum_{m=1}^M F_m^{(V)}(q), \quad (7)$$

where  $N_m^{(V)} = \sum_{e=1}^E n_{me}$  is the sum of multiplicities which appear in the  $m$ th bin of all events.

Besides the horizontal and vertical factorial moment methods, a mixed approach is applied. Mixed factorial moments are defined as

$$F^{(HV)}(q) = \frac{1}{M} \sum_{m=1}^M \frac{\frac{1}{E} \sum_{e=1}^E F(n_{me}; q)}{\left[ \frac{1}{M} \frac{1}{E} \sum_{e=1}^E N_e^{(H)} \right]^q} = M^{q-1} E^{q-1} \frac{\sum_{m=1}^M \sum_{e=1}^E F(n_{me}; q)}{[N^{(HV)}]^q}, \quad (8)$$

where  $N^{(HV)} = \sum_{m=1}^M \sum_{e=1}^E n_{me}$  is the total number of charged particles observed in the sample of  $E$  events.

For experimental data of Si + Ag(Br) interactions at 14.6 A GeV/c, we used all the three above-mentioned methods of analysis — HFM, VFM and MFM. The  $\ln \langle F_q \rangle$  dependences on  $\ln M$  have been obtained. The results of this analysis have been published in [19]. The values of slopes are given in Table 1. The

**Table 1. The values of slopes for 14.6 A GeV/c  $^{28}\text{Si}$  events in  $\eta$  space for  $q = 2-5$  using HFM, VFM and MFM methods**

| Method | $\varphi_2$       | $\varphi_3$       | $\varphi_4$       | $\varphi_5$       |
|--------|-------------------|-------------------|-------------------|-------------------|
| HFM    | $0.037 \pm 0.005$ | $0.076 \pm 0.012$ | $0.112 \pm 0.021$ | $0.145 \pm 0.032$ |
| VFM    | $0.030 \pm 0.004$ | $0.099 \pm 0.018$ | $0.188 \pm 0.076$ | $0.228 \pm 0.088$ |
| MFM    | $0.034 \pm 0.002$ | $0.071 \pm 0.005$ | $0.114 \pm 0.014$ | $0.171 \pm 0.034$ |

values of slopes  $\varphi_q$  obtained by all these methods are similar for  $q = 2-5$ , where  $q$  is the order of factorial moment. Because all the three methods give similar values of slopes, in next analysis we used the HFM method only.

From the total number of 628 measured events of  $^{208}\text{Pb} + \text{Em}$  interactions at 158 A GeV/c, 64 collisions with the number of relativistic particles  $N_s > 350$

have been selected. The interactions with  $N_s > 350$  are those of lead nuclei with heavy emulsion targets (Ag, Br) [13]. The interactions with increasing number of relativistic particles or degree of centrality, respectively, have also been studied (see Table 2).

The  $\ln \langle F_q \rangle$  dependences on  $\ln M$  (for  $q = 2-6$ ) have been obtained by horizontal factorial moment method. Some results of this analysis have been published in our previous work [20]. The dependence of  $\ln \langle F_q \rangle$  on  $\ln M$  for Pb+Ag(Br) interactions with  $N_s > 1000$  obtained by HFM is shown in Fig. 10.

In our next analysis the dependences of parameters  $\alpha_q$  and  $\varphi_q$  ( $\ln \langle F_q \rangle = \alpha_q + \varphi_q \ln M$ ) on the order of factorial moments  $q$  have been studied for  $\Delta\eta = 0-7.4$  and  $M = 7-74$ . In Fig. 11 the increasing dependences of values of slopes ( $\varphi_q$ ) on  $q$  for two groups ( $N_s > 350$ ,  $N_s > 1000$ ) of Pb induced interactions in emulsion are shown. The steepest dependence of values of slopes on  $q$  has been found for interactions with  $N_s > 1000$ . These dependences ( $\varphi_q > 0$ ) show an evidence for the presence of intermittent behaviour or nonstatistical fluctuations. Figure 12 presents the dependence of intercept parameter  $\alpha_q$  on  $q$  for the most central Pb interactions,  $q = 2-6$ .

For comparison we used other experimental data obtained by the same standard emulsion method. The characteristics of used experimental data — beam nucleus, momentum ( $p$ ), number of bins ( $M$ ) and bin size ( $\delta\eta$ ) of relativistic particles — are given in Table 3.

In Fig. 13 is shown our new result — the dependences of slope  $\varphi_q$  on  $q$  for Pb+Em and Au+Em central interactions. Measurements and calculations have been done in similar conditions: similar masses of projectiles and similar

**Table 2. Different groups of  $^{208}\text{Pb}$  interactions in emulsion.  $N_i$  is number of interactions,  $\langle N_s \rangle$  is average number of relativistic particles**

|              | $N_i$ | $\langle N_s \rangle$ |
|--------------|-------|-----------------------|
| $N_s > 350$  | 64    | 635                   |
| $N_s > 400$  | 52    | 698                   |
| $N_s > 500$  | 40    | 775                   |
| $N_s > 600$  | 35    | 809                   |
| $N_s > 700$  | 23    | 900                   |
| $N_s > 800$  | 14    | 993                   |
| $N_s > 900$  | 8     | 1097                  |
| $N_s > 1000$ | 7     | 1120                  |

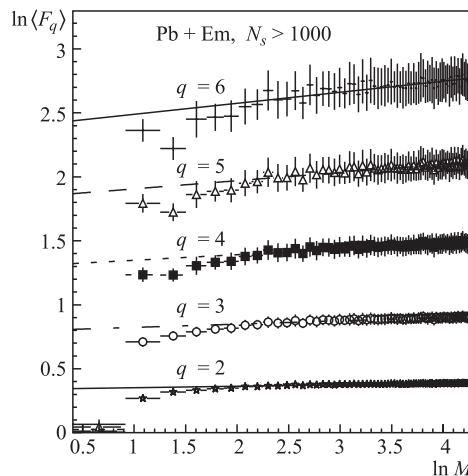


Fig. 10. The dependence of  $\ln \langle F_q \rangle$  on  $\ln M$  for Pb+Ag(Br) interactions with  $N_s > 1000$ ,  $q = 2-6$ , obtained by HFM

**Table 3. Experimental data**

| Beam nucleus  | $^{16}\text{O}$ | $^{16}\text{O}$ | $^{197}\text{Au}$ | $^{208}\text{Pb}$ |
|---------------|-----------------|-----------------|-------------------|-------------------|
| $p$ , A GeV/c | 60              | 200             | 11.6              | 158               |
| $M$           | 6–64            | 8–76            | 4–25              | 7–74              |
| $\delta\eta$  | 1.07–0.1        | 0.95–0.1        | 1.25–0.2          | 1.057–0.1         |

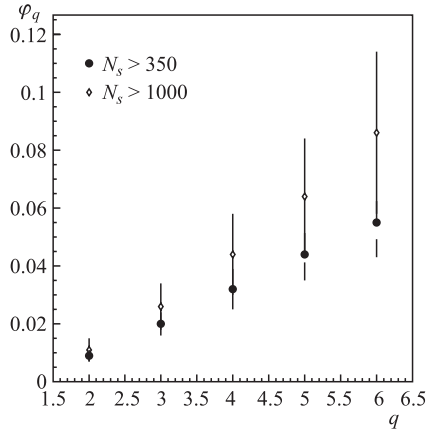


Fig. 11. The  $\varphi_q$  dependences on  $q$  ( $q = 2-6$ ) for Pb+Em interactions with  $N_s > 350$  and  $N_s > 1000$ ,  $\Delta\eta = 0-7.4$ ,  $M = 7-74$

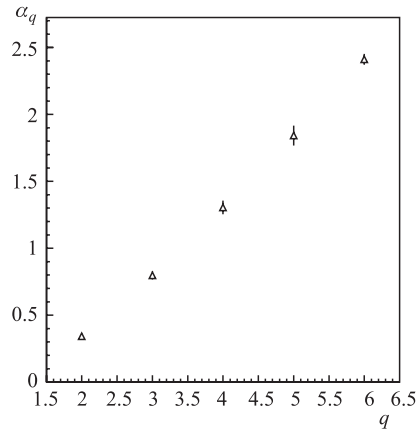


Fig. 12. The  $\alpha_q$  dependence on  $q$  ( $q = 2-6$ ) for Pb+Em interactions with  $N_s > 1000$ ,  $\Delta\eta = 0-7.4$ ,  $M = 7-74$

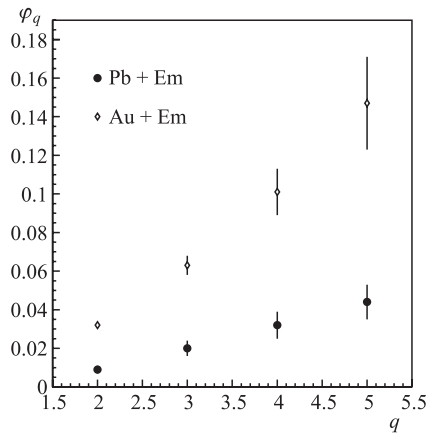


Fig. 13. The  $\varphi_q$  dependence on  $q$  ( $q = 2-5$ ) for Pb+Em and Au+Em central interactions with  $N_s > 350$  and  $N_s > 100$ , respectively

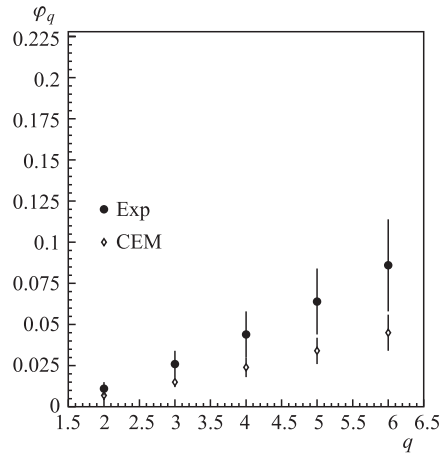


Fig. 14. The  $\varphi_q$  on  $q$  for Pb experimental and CEM data at 158 A GeV/c  $N_s > 1000$

**Table 4. The values of slopes for experimental data from 4.5 A GeV/c and 14.6 A GeV/c  $^{28}\text{Si}$  events in  $\eta$  space for  $q = 2-5$ , the values in the brackets are from CEM data**

| Energy       | $\varphi_2$                                | $\varphi_3$                                | $\varphi_4$                                | $\varphi_5$                                |
|--------------|--|--|--|--|
| 4.5 A GeV/c  | $0.044 \pm 0.009$<br>( $0.008 \pm 0.004$ ) | $0.117 \pm 0.025$<br>( $0.023 \pm 0.012$ ) | $0.224 \pm 0.051$<br>( $0.032 \pm 0.023$ ) | $0.336 \pm 0.092$<br>( $0.040 \pm 0.037$ ) |
| 14.6 A GeV/c | $0.037 \pm 0.005$<br>( $0.023 \pm 0.003$ ) | $0.076 \pm 0.012$<br>( $0.045 \pm 0.008$ ) | $0.112 \pm 0.021$<br>( $0.063 \pm 0.014$ ) | $0.145 \pm 0.032$<br>( $0.076 \pm 0.021$ ) |

**Table 5. The values of slopes for experimental data from 4.5 A GeV/c and 14.6 A GeV/c  $^{16}\text{O}$  events in  $\eta$  space for  $q = 2-5$ , the values in the brackets are from CEM data at the same momenta**

| Energy       | $\varphi_2$                                | $\varphi_3$                                | $\varphi_4$                                | $\varphi_5$                                |
|--------------|--|--|--|--|
| 4.5 A GeV/c  | $0.041 \pm 0.006$<br>( $0.018 \pm 0.003$ ) | $0.099 \pm 0.015$<br>( $0.035 \pm 0.004$ ) | $0.178 \pm 0.029$<br>( $0.050 \pm 0.019$ ) | $0.270 \pm 0.048$<br>( $0.072 \pm 0.033$ ) |
| 14.6 A GeV/c | $0.040 \pm 0.004$<br>( $0.018 \pm 0.004$ ) | $0.094 \pm 0.017$<br>( $0.026 \pm 0.009$ ) | $0.163 \pm 0.031$<br>( $0.021 \pm 0.016$ ) | $0.236 \pm 0.047$<br>( $0.017 \pm 0.025$ ) |

values of bin size ( $\delta\eta = 0.1-1.057$  for Pb + Em and  $\delta\eta = 0.2-1.25$  for Au + Em). The central events have been selected for this analysis only, i.e., Pb events with  $N_s > 350$  and Au events with  $N_s > 100$ . A similar trend of  $\varphi_q$  dependences on  $q$  only for Pb + Em data was published in [21].

The results of analysis using HFM method have been compared with the values obtained from data sample calculated by the modified cascade-evaporation model (CEM). The description of CEM can be found in [10]. The values of slopes obtained by HFM for the experimental data of  $^{28}\text{Si}$  interactions at 14.6 A GeV/c and 4.5 A GeV/c are given in Table 4 [19]. The values in the brackets are from CEM data at the same momenta. The similar comparison for  $^{16}\text{O}$  + Em experimental and CEM data at 4.5 and 14.6 A GeV/c are given in Table 5. These results have been published in our previous work [22]. One can see that the values of slopes for experimental samples are higher than the values calculated using CEM.

The events of Pb + Ag(Br) with  $N_s > 1000$  have also been studied. The  $\varphi_q$  dependences on  $q$  for Pb + Ag(Br) experimental and CEM data are presented in Fig. 14.

The values of slopes for experimental data are higher than the values from CEM. Similar results have been published by B. Wosiek in [21] for Pb + Em and MC calculations at 158 A GeV/c, where the slopes  $\varphi_q$  increase with increasing value of  $q$  and values of slopes are higher than those obtained from MC calculations.

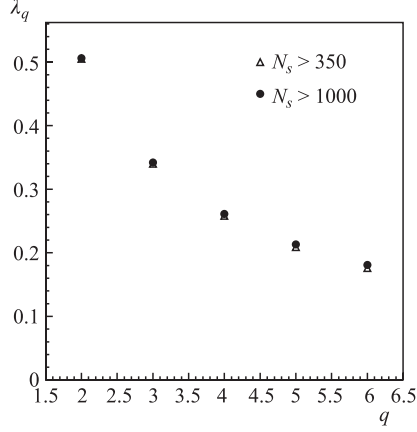


Fig. 15. The dependence of intermittency parameter ( $\lambda_q$ ) on  $q$  ( $q = 2-6$ ) for Pb interactions with  $N_s > 350$  and  $N_s > 1000$

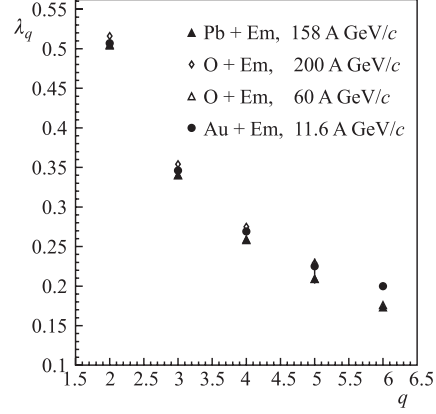


Fig. 16. The dependence of intermittency parameter ( $\lambda_q$ ) on  $q$  ( $q = 2-6$ ) for different primary nuclei

The dependences of intermittency parameter ( $\lambda_q$ ) on the order of factorial moment  $q$  have been studied. The intermittency parameter is defined as

$$\lambda_q = \frac{\varphi_q + 1}{q}. \quad (9)$$

If the function  $\lambda_q$  on  $q$  had a minimum at a certain  $q = q_c$ , there would be a possibility of observing a nonthermal phase transition [23, 24].

The dependences of intermittency parameter ( $\lambda_q$ ) on the order of factorial moment  $q$  for two groups of Pb interactions with different degree of centrality ( $N_s > 350$  and  $N_s > 1000$ ) are presented in Fig. 15. No minimum of  $\lambda_q$  dependence on  $q$  has been found. Similar dependences for  $\delta\eta = 0.1-3.7$  have been published in [20], no minimum of  $\lambda_q$  on  $q$  has also been found.

The dependences of intermittency parameter ( $\lambda_q$ ) on the order of factorial moment  $q$  for different primary nuclei have been studied. In Fig. 16 the  $\lambda_q$  dependences on the order of factorial moment  $q$  for different experimental data samples (see Table 3) are presented, but no minimum has been found. There are some hints for existence of minima at  $q_c = 4-5$  published in [24, 25].

The dependence of values of slopes  $\varphi_2$  on particle density per unit pseudorapidity  $\rho$  has been studied using different primary nuclei. Our preliminary result obtained for interval bin size  $\delta\eta \sim 0.1-1.25$  (in logarithmic scale) is shown in Fig. 17. Similar results for chamber emulsion data in pseudorapidity interval  $0.09 < \delta\eta < 2$  have been published in [26].

Central interactions of  $^{208}\text{Pb}$  nuclei at 158 A GeV/c in emulsion have been analyzed using the horizontal factorial moment method. The scaled factorial moments  $F_q$  of the order  $q$  have been studied as a function of the pseudorapidity bin size, parametrized in the form  $\ln \langle F_q \rangle = \alpha_q + \varphi_q \ln M$ . An evidence for the presence of intermittent behaviour has been shown. The dependences of parameters  $\alpha_q$  and  $\varphi_q$  on the order of factorial moments  $q$  have been studied. The comparison for different primary nuclei ( $^{16}\text{O}$  at momenta of 4.5–200 A GeV/c and  $^{197}\text{Au}$  at 11.6 A GeV/c) has been done. The dependences of intermittency parameter  $\lambda_q$  on  $q$  for different primary nuclei have been studied, but no clear minimum has been found.

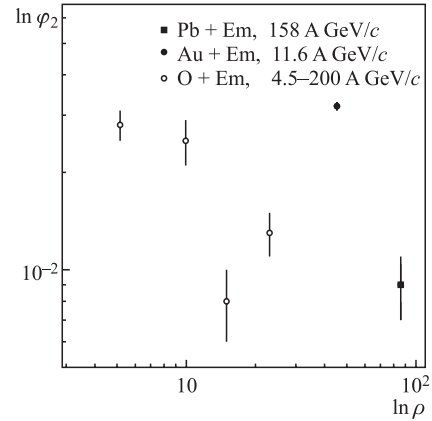


Fig. 17. The dependence of  $\ln \varphi_2$  on  $\ln \rho$ ;  $\rho$  is particle density per unit pseudorapidity

#### 4. CONCLUSION

Emission of relativistic particles produced in central  $^{208}\text{Pb}$  induced nuclear collisions at 158 A GeV/c has been studied using three different approaches — scaled factorial moments, wavelets and parameter  $S_2$ .

- An evidence for nonstatistical fluctuations has been shown using horizontal factorial moment method in pseudorapidity phase space. The comparative study has been done for different beam energies and masses and for different centrality selection of Pb events. No clear minimum has been found in the dependences of intermittency parameter  $\lambda_q$  on  $q$ .
- In the wavelet analysis some irregularities have been observed mainly in the scale range  $a \leq 0.5$ , which indicate the preferred pseudorapidities of groups of emitted particles.
- When the azimuthal structures of produced particles have been investigated using the  $S_2$  method, the additional groups of produced particles in the region of the ring-like structures ( $S_2/\langle S_2 \rangle < 1$ ) and the jet-like structures ( $S_2/\langle S_2 \rangle > 1$ ) in comparison to the FRITIOF model calculations have been observed.

**Acknowledgments.** Financial support from the Scientific Agency of the Ministry of Education of the Slovak Republic and the Slovak Academy of Sciences (Grant No. 1/0080/08) is cordially acknowledged.

## REFERENCES

1. E. Stenlund et al., Nucl. Phys. **A498**, 1989, p.541c.
2. L. Van Hove, Z. Phys. **C21**, 1984, p.93.
3. M.I. Adamovich et al., J. Phys. G: Nucl. Part. Phys. **19**, 1993, p.2035.
4. V. Uzhinsky et al., JINR Preprint P1-2001-119, Dubna, 2001.
5. M. Blažek, Int. Journal of Mod. Phys. **A12**, 1997, p.839.
6. A.S. Gaitinov et al., Proc. of the XVII Meeting of the EMU01 Collaboration, Dubna, Russia, May 18–20, 1999, Dubna, 2000, p.143.
7. M.I. Adamovich et al., Eur. Phys. J. **A5**, 1999, p.429.
8. B. Nilsson-Almqvist, E. Stenlund, Comp. Phys. Com. **43**, 1987, p.387.
9. V. Uzhinsky, JINR Preprint E2-96-192, Dubna, 1996.
10. G. Musulmanbekov, JINR Preprint P-2-99-59, Dubna, 1999; also in: AIP, 1995, 428.1
11. S. Vokál S. et al., Physics of Atomic Nuclei **71**, 2008, p.1395.
12. G.I. Orlova, A. Kravčáková, S. Vokál, V.V. Prosin, Proc. of the Hadron Structure 2002, Herľany, Sept. 22–27, 2002, Košice, 2003, p.155.
13. S. Vokál et al., JINR Preprint E1-2004-173, Dubna, 2004.
14. S. Vokál, S. Lehocká, G.I. Orlova, JINR Preprint E1-2005-66, Dubna, 2005.
15. J. Fedorišin, S. Vokál, JINR Preprint E1-2007-4, Dubna, 2007.
16. J. Fedorišin, S. Vokál, JINR Preprint E1-2007-66, Dubna, 2007.
17. A. Bialas, R. Peschanski, Nucl. Phys. **B273**, 1986, p.703.
18. A. Bialas, R. Peschanski R, Nucl. Phys. **B308**, 1988, p.857.
19. M.I. Adamovich et al., APH N.S., Heavy Ion Physics **13**, 2001, p.213.
20. J. Vrláková, S. Vokál, A. Dirner, Acta Physica Slovaca **56**, 2006, p.83.
21. B. Wosiek, Acta Physica Slovaca **46**, 1996, p.531.
22. J. Vrláková, S. Vokál, Zborník príspevkov 14. konf. slov. a českých fyzikov, Plzeň, 9–12.9. 2002, ZU Plzeň, ČR, 2002, p.178.
23. A. Bialas, K. Zalewski, Phys. Lett. **B238**, 1990, p.413.
24. D. Ghosh et al., Europhys. Lett. **41**, 1998, p.371.
25. E.K. Sarkisyan et al., Phys. Lett. **B347**, 1995, p.439.
26. R.J. Wilkes et al. (EMU01 col.), Nucl. Phys. **A544**, 1992, p.153c.

Received on December 8, 2009.